Arch Toxicol
DOI 10.1007/s00204-013-1045-1

BIOLOGICALS

# In vitro characterisation of the anti-intravasative properties of the marine product heteronemin

**Sabine Kopf · Katharina Viola · Atanas G. Atanasov · Kanokwan Jarukamjorn · Lucie Rarova · Nicole Kretschy · Mathias Teichmann · Caroline Vonach · Philipp Saiko · Benedikt Giessrigl · Nicole Huttary · Ingrid Raab · Sigurd Krieger · Marc Schumacher · Marc Diederich · Miroslav Strnad · Rainer de Martin · Thomas Szekeres · Walter Jäger · Verena M. Dirsch · Wolfgang Mikulits · Michael Grusch · Helmut Dolznig · Georg Krupitza**

Received: 5 December 2012 / Accepted: 19 March 2013


**Abstract** Metastases destroy the function of infested organs and are the main reason of cancer-related mortality. Heteronemin, a natural product derived from a marine sponge, was tested in vitro regarding its properties to prevent tumour cell intravasation through the lymph-endothelial barrier. In three-dimensional (3D) cell cultures consisting of MCF-7 breast cancer cell spheroids that were placed on lymph-endothelial cell (LEC) monolayers, tumour cell spheroids induce "circular chemorepellent-induced defects" (CCIDs) in the LEC monolayer; 12(S)-Hydroxyeicosatetraenoic acid (12(S)-HETE) and NF-κB activity are major factors inducing CCIDs, which are entry gates for tumour emboli intravasating the vasculature. This 3D co-culture is a validated model for the investigation of intravasation mechanisms and of drugs preventing CCID formation and hence lymph node metastasis. Furthermore, Western blot analyses, NF-κB reporter, EROD, SELE, 12(S)-HETE, and adhesion assays were performed to investigate the properties of heteronemin. Five micromolar heteronemin inhibited the directional movement of LECs and, therefore, the formation of CCIDs, which were induced by MCF-7 spheroids. Furthermore, heteronemin reduced the adhesion of MCF-7 cells to LECs and suppressed 12(S)-HETE-induced expression of the EMT marker paxillin, which is a regulator of directional cell migration. The activity of CYP1A1, which contributed to

S. Kopf · K. Viola · N. Kretschy · M. Teichmann · C. Vonach · B. Giessrigl · N. Huttary · I. Raab · S. Krieger · G. Krupitza (✉)
Institute of Clinical Pathology, Medical University of Vienna, Waehringer Guertel 18-20, 1090 Vienna, Austria
e-mail: georg.krupitza@meduniwien.ac.at

A. G. Atanasov · V. M. Dirsch
Department of Pharmacognosy, University of Vienna, Althanstrasse 14, 1090 Vienna, Austria

K. Jarukamjorn · W. Jäger
Department for Clinical Pharmacy and Diagnostics, Faculty of Life Sciences, University of Vienna, Althanstrasse 14, 1090 Vienna, Austria

K. Jarukamjorn
Department of Pharmaceutical Chemistry, Faculty of Pharmaceutical Sciences, Khon Kaen University, Khon Kaen 40002, Thailand

L. Rarova · M. Strnad
Faculty of Science, Centre of the Region Haná for Biotechnological and Agricultural Research, Palacký University, Šlechtitelů 11, 783 71 Olomouc, Czech Republic

P. Saiko · T. Szekeres
Department of Medical and Chemical Laboratory Diagnostics, General Hospital of Vienna, Medical University of Vienna, Waehringer Guertel 18-20, 1090 Vienna, Austria

M. Schumacher · M. Diederich
Laboratoire de Biologie Moléculaire et Cellulaire du Cancer, Hôpital Kirchberg, 9 Rue Edward Streichen, 2540 Luxembourg, Luxembourg

R. de Martin
Department of Vascular Biology and Thrombosis Research, Medical University of Vienna, Lazarettgasse 19, 1090 Vienna, Austria

W. Mikulits · M. Grusch
Department of Medicine I, Institute of Cancer Research, Medical University of Vienna, Borschkegasse 8a, 1090 Vienna, Austria

H. Dolznig
Institute of Medical Genetics, Medical University of Vienna, Währinger Strasse 10, 1090 Vienna, Austria

Published online: 30 March 2013

CCID formation, was also inhibited by heteronemin. Hence, heteronemin inhibits important mechanisms contributing to tumour intravasation in vitro and should be tested in vivo.

**Keywords** Heteronemin · Intravasation · Lymph endothelium · Adhesion · Mobility

**Abbreviations**

| | |
|---|---|
| ALOX | Lipoxygenase A |
| CCIDs | Circular chemorepellent-induced defects |
| CYP | Cytochrome P450 |
| EMT | Epithelial to mesenchymal transition |
| EROD | Ethoxyresorufin-*O*-deethylase |
| HUVEC | Human umbilical vein endothelial cell |
| ICAM-1 | Intercellular adhesion molecule 1 |
| LEC | Lymph-endothelial cell |
| MCL2 | Myosin light chain 2 |
| SELE | Selectin E |
| 12(S)-HETE 12(S) | Hydroxyeicosatetraenoic acid |

## Introduction

Breast cancer is the major cause for cancer death of women in the western hemisphere. The fatal outcome is due to the destruction of the integrity and function of organs by distant metastases. The route by which metastases travel to colonise distant organs is the lymphatic vasculature, and the status of tumour cell infested lymph nodes is predictive for survival and commonly used for routine diagnosis (Carlson et al. 2009; Sobin et al. 2009). Intravasation of tumour cells into the vasculature depends on cell attachment and on the motility of tumour cells and endothelial cells. The interactive process of intravasation of breast cancer cells into the lymphatic vasculature was recently unravelled. A three-dimensional (3D) co-culture system consisting of MCF-7 breast cancer cell spheroids and telomerase-immortalised human lymph-endothelial cell (LEC) monolayers, which faithfully resembles the clinical situation of lymph node metastasis, was established (Kerjaschki et al. 2011; Madlener et al. 2010; Schoppmann et al. 2004). Therefore, this 3D co-culture model allows to mechanistically dissect processes of tumour cell intravasation into lymphatics. In case of metastasising ductal breast cancer, one intravasation mechanism is the activation of ALOX12/15 and the secretion of its metabolite 12(S)-hydroxyeicosatetraenoic acid [12(S)-HETE] by cancer cells. ALOX12, which is the major enzyme producing 12(S)-HETE, plays a role in tumour promotion, progression, and metastasis (Nie et al. 2003; Nie and Honn 2004; Yoshimura et al. 2004) and was described as "endothelial retraction factor" (Honn et al. 1994). Therefore, 12(S)-HETE, which is secreted by MCF-7 cells (Uchide et al. 2007), triggers the formation of so-called circular chemorepellent-induced defects (CCIDs) in the adjacent LEC monolayer through enhanced LEC mobility as a prerequisite for LEC retraction (Kerjaschki et al. 2011). CCIDs are considered as gates for tumour bulks entering the lymphatic vasculature.

The specific ALOX12/15 inhibitor baicalein was proposed as a promising compound in the fight against cancer (Leung et al. 2007), and in fact, baicalein inhibits the formation of CCIDs when MCF-7 spheroids are pre-treated in the 3D model (Madlener et al. 2010; Kerjaschki et al. 2011; Viola et al. 2013a). Normally, 12(S)-HETE is mainly produced by platelets, leucocytes, smooth muscle, epithelium, neuron, and fibroblast cells (Spector et al. 1988) and induces not only the retraction of microvascular endothelial cells, but it also increases tumour cell adhesion to exposed ECM (Tang et al. 1993; Honn et al. 1994). Increased adhesion to tumour cells enhances LEC plasticity due to the activation of proteins co-migrating with myosin light chain (Rice et al. 1998), actin, and vimentin (Tang et al. 1993) and other molecules regulating mobility (Viola et al.

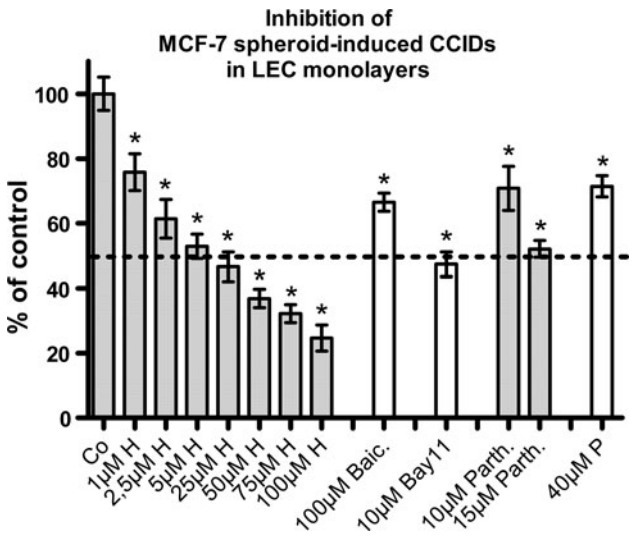


**Fig. 1** Effect of heteronemin on the size of circular chemically induced defects (CCIDs) in LECs triggered by MCF-7 cell spheroids. MCF-7 spheroids and LEC monolayers were pre-treated for 30 min with 1, 2.5, 5, 25, 50, 75, and 100 µM heteronemin (H), or 100 µM baicalein (Baic.), 10 µM Bay11-7082 (Bay11), 10 and 15 µM parthenolide (Parth.), or 40 µM proadifen (P). Then, MCF-7 spheroids were placed on top of LEC monolayers and co-cultivated for 4 h. As control (Co), CCIDs of untreated co-cultures were measured. The CCIDs underneath 12 spheroids were analysed for each condition. Experiments were performed in triplicate; *error bars* indicate mean ± SEM and *asterisks* significance ($p < 0.05$)

2013a). The acquisition of a more mobile and mesenchymal phenotype of LECs and the formation of CCIDs can be caused by the deregulation of NF-κB, which is associated with cancer development (Folmer et al. 2009) and the promotion of oncogenesis through the transcriptional activation of genes associated with cell proliferation, angiogenesis, apoptosis, and metastasis (Orlowski and Baldwin 2002). The intravasation of tumour emboli through the lymph-vascular barrier is attenuated by the inhibition of NF-κB, thereby inhibiting "epithelial to mesenchymal transition" (EMT) (Vonach et al. 2011).

Novel drugs are needed in cancer therapy particularly to inhibit metastatic spread. Besides mechanistic studies, the 3D intravasation model can also be used to discover and functionally investigate new compounds with anti-metastatic activity. Currently, about 60 % of all drugs used in western medicine derive from natural compounds (Cragg et al. 2006). Therefore, we tested heteronemin which was isolated from marine sponges (i.e. *Hyrtios* sp., *Brachiaster* sp.; Kobayashi et al. 1994; Wonganuchitmeta et al. 2004) and which was shown to inhibit NF-κB (Schumacher et al. 2010), regarding its properties to inhibit tumour cell adhesion, LEC plasticity, and CCID forming mechanisms.

## Materials and methods

### Reagents and antibodies

The NF-κB inhibitor parthenolide, the I-κBα phosphorylation inhibitor (E)-3-[(4-methylphenyl-sulfonyl]-2-propenenitrile (Bay11-7082), and the ALOX12/15 inhibitor baicalein (EI-106) were purchased from Biomol (Hamburg, Germany), 12(S)-HETE from Cayman Chemical (Ann Arbor, MI, USA), and proadifen (SKF-525A) from Sigma-Aldrich (Munich, Germany). Mouse monoclonal anti-CD54 (ICAM-1) antibody was from Immunotech (Marseille, France) and polyclonal rabbit anti-paxillin (H-114) (SC-5574) and β-tubulin (H-235, sc-9104) from Santa Cruz Biotechnology (Heidelberg, Germany). Monoclonal mouse anti-phospho-p44/42 MAPK (Erk1/2) (Thr202/Tyr204) (E10), monoclonal rabbit anti-p44/42 MAPK (Erk1/2) (137F5), and polyclonal rabbit anti-MYPT1 were from Cell Signaling (Danvers, MA, USA). Monoclonal mouse anti-β-actin (clone AC-15) and polyclonal rabbit anti-S100A4 were from Sigma-Aldrich (Munich, Germany) and polyclonal rabbit anti-phospho-MYPT1 (Thr696) from Upstate (Lake Placid, NY, USA). Monoclonal mouse anti-CD31 (JC70A), polyclonal rabbit anti-mouse, and anti-rabbit IgGs were from Dako (Glostrup, Denmark).

### Cell culture

Human MCF-7 breast cancer cells were purchased from the American Type Culture Collection (ATCC, Rockville, MD, USA) and grown in MEM medium supplemented with 10 % foetal calf serum (FCS), 1 % penicillin/streptomycin (PS) (Invitrogen, Karlsruhe, Germany). Telomerase immortalised human lymph-endothelial cells (LECs) were grown in EGM2 MV (Clonetics CC-4147, Allendale, NJ, USA), all at 37 °C in a humidified atmosphere containing 5 % $CO_2$. For CCID formation assays, LECs were stained with cytotracker green purchased from Invitrogen (Karlsruhe, Germany). Human umbilical vein endothelial cells (HUVECs) were isolated and cultured in M199 medium supplemented with 20 % FCS, antibiotics, endothelial cell growth supplement and heparin as previously described (Zhang et al. 1998).

Three-dimensional co-cultivation of breast cancer spheroids with LEC monolayers: MCF-7 cells were transferred to 30 ml MEM medium containing 6 ml of a 1.6 % methylcellulose solution (0.3 % final concentration; Cat. No.: M-512, 4000 centipoises; Sigma-Aldrich, Munich, Germany); 150 µl of this cell suspension was transferred to each well of a 96-well plate (Greiner Bio-one, Cellstar 650185, Kremsmünster, Austria) to allow spheroid formation within 48 h. Then, MCF-7 spheroids were washed in PBS and transferred to cytotracker-stained LEC monolayers that were seeded into 24-well plates (Costar 3524, Sigma-Aldrich, Munich, Germany) in 2 ml EGM2 MV medium.

**Table 1** Heteronemin inflammation assay

| Analysis | | Control | TNFα | TNFα & 1 µM H | TNFα & 5 µM H | TNFα & 10 µM H |
|---|---|---|---|---|---|---|
| SELE expression in TNFα-induced HUVECs | | | | | | |
| Inflammatory reaction | SELE | 0.051 | 0.145 | 0.155 | 0.151 | 0.146 |
| | (OD) | SD 0.004 | SD 0.011 | SD 0.003 | SD 0.017 | SD 0.003 |
| Cytotoxicity | Calcein AM | 47.6 | 47.8 | 48.8 | 52.4 | 48.4 |
| | (OD) | SD 4.0 | SD 5.7 | SD 2.3 | SD 2.2 | SD 4.9 |

$1 \times 10^4$ HUVECs/well were seeded into 96-well plates and grown to confluence. Indicated concentrations of heteronemin (H) were added 30 min prior to application of 10 ng/ml TNFα for another 4 h. Then, cells were fixed and SELE levels analysed by ELISA. In parallel, extracts were analysed by Calcein AM assay to monitor non-specific extract toxicity

During the experiments, which were mostly short term, we did not observe toxic effects of heteronemin (monitored by HOPI staining; Grusch et al. 2002).

### CCID assay

In this model, the sizes of the cell-free areas (circular chemorepellent-induced defects, CCIDs) are measured, which are formed in the endothelial monolayer directly underneath the tumour spheroids (Viola et al. 2013a, b; Giessrigl et al. 2012; Vonach et al. 2011; Kerjaschki et al. 2011; Madlener et al. 2010). MCF-7 cell spheroids (3,000 cells/spheroid) were transferred to 24-well plates containing LEC monolayers. After 4 h of incubation, the CCID areas in the LEC monolayers underneath the MCF-7 spheroids were photographed using an Axiovert (Zeiss, Jena, Germany) fluorescence microscope to visualise cytotracker (green)-stained LECs underneath the spheroids. CCID areas were calculated with the Axiovision Re. 4.5 software (Zeiss, Jena, Germany). MCF-7 spheroids were treated with the indicated compounds or solvent (DMSO) as negative control. Each experiment was performed in triplicate, and for each condition, the CCID size of 12 or more spheroids (unless otherwise specified) was measured.

### SDS gel electrophoresis and Western blotting

Lymph-endothelial cells were grown in petri dishes (6 cm diameter) to 80 % confluence and treated with 1 µM 12(S)-HETE and/or 5 µM heteronemin. Then, cells were washed twice with cold PBS and lysed in a buffer containing 150 mM NaCl, 50 mM Tris pH 8.0, 1 % Triton-X-100, 1 mM phenylmethylsulfonyl fluoride (PMSF), and 1 mM protease inhibitor cocktail (PIC), (Sigma, Schnelldorf, Germany). The lysate was centrifuged at 12,000 rpm for 20 min at 4 °C. Supernatant was transferred into a 1.5-ml tube and stored at −20 °C until further analysis. Equal amounts of protein lysate were mixed with SDS (sodium dodecyl sulphate) sample buffer and loaded onto a 10 % polyacrylamide gel. SDS polyacrylamide gel electrophoresis (PAGE) and Western blotting were used according to the protocol described by Vonach et al. (2011).

### SELE (CD62E, E-selectin, ELAM)-induction assay

Each well of a 96-well plate was coated with gelatine by applying 200 µl of 1.0 % gelatine for 10 min at room temperature. Outer wells (A1-A12, H1-H12, 1-H1, and A12-H12) contained only 200 µl/well medium and served as an evaporation barrier;. $1 \times 10^4$ HUVECs were seeded in each of the other wells in 200 µl medium and grown for 48 h to confluence. Increasing concentrations of heteronemin were then added to the HUVEC-containing wells in triplicates, and the cells were incubated for 30 min, after which 10 ng/ml TNFα was added per well to stimulate NF-κB and thus SELE. After further 4 h of incubation, the levels of SELE in each of the HUVEC-containing wells were determined by enzyme-linked activity assays (ELISAs) as described below.

#### *Cellsurface ELISA SELE*

Cells were washed once with PBS and fixed with 0.1 % glutaraldehyde (Sigma-Aldrich, Munich, Germany), for 15 min at room temperature. Then, cells were washed 3× with 200 µl per well PBS/0.05 % Tween 20, blocked with 200 µl/well 5 % BSA/PBS for 1 h, and washed again 3× with 200 µl per well PBS/0.05 % Tween 20. Then, anti-SELE antibody (clone BBA-1, R&D Systems, Minneapolis, MN, USA) diluted 1:5000 in 0.1 % BSA/PBS (100 µl per well) was added for 1 h at room temperature and washed thereafter 5× with 200 µl per well PBS/0.05 % Tween 20. Subsequently, goat anti-mouse-HRP antibody (Sigma-Aldrich, Munich, Germany) diluted 1:10000 in 0.1 % BSA/PBS (100 µl per well) was applied, and the cells were incubated for a further hour in the dark at room temperature and, after decanting, washed 5× with 200 µl per well PBS/0.05 % Tween 20. The HRP activity of the cells in each of the wells was estimated using Fast OPD (*o*-phenylenediamine dihydrochloride) (Sigma-Aldrich, Munich, Germany) assay as described by (Gridling et al. 2009), and absorbance was measured at $OD_{492nm}$ in a vertical spectrophotometer.

#### *Cytotoxicity testing*

For the SELE expression assay, the toxicity of heteronemin was assessed in HUVECs by Calcein AM cytotoxicity assays in 96-well microtitre plates (Madlener et al. 2009). Twenty microlitre portions of each of the heteronemin concentrations were added in triplicate to the cells, which were then incubated at 37 °C in an atmosphere containing 5 % $CO_2$ for 4 h, after which Calcein AM solution (Molecular Probes, Invitrogen, Karlsruhe, Germany) was added for 1 h according to the manufacturer's instructions. The fluorescence of viable cells was quantified using a Fluoroskan Ascent instrument (Labsystems, Finland) reader, and on the basis of triplicate experiments, the cytotoxic concentrations were calculated.

### NF-κB luciferase assay

$1 \times 10^7$ HEK293-NF-κB-Luc cells (Panomics, Fremont, USA) were seeded in 20 ml full growth DMEM medium in a 15-cm dish. Next day, cells were transfected with an expression plasmid for green fluorescence protein

(pEGFP-N1; Clontech, CA, USA). A total of 30 µl Lipofectamine 2000 (Invitrogen, Karlsruhe, Germany) and 7.5 µg DNA were mixed in 2 ml transfection medium and incubated for 20 min at room temperature followed by adding this mixture to the cells. After incubation for 6 h in humidified atmosphere containing 5 % $CO_2$, $4 \times 10^4$ cells per well were seeded in serum- and phenol red-free DMEM in a 96-transparent-well plate. On the next day, cells were treated with 2.5, 5, and 10 µM heteronemin and 2.5 µM parthenolide as a specific inhibitor of NF-κB (control). One hour after treatment, cells were stimulated with 2 ng/ml human recombinant TNFα for additional 4 h. Luminescence of the firefly luciferase and fluorescence of the GFP were quantified on a GeniusPro plate reader (Tecan, Grödig, Austria). The luciferase signal derived from the NF-κB reporter was normalised by the GFP-derived fluorescence to account for differences in cell number or transfection efficiency (Giessrigl et al. 2012).

### Ethoxyresorufin-*O*-deethylase (EROD) assay selective for CYP1A1 activity

MCF-7 breast cancer cells were grown in phenol red-free RPMI 1640 tissue culture medium (PAN Biotech, Aldenbach, Germany), supplemented with 10 % FCS and 1 % PS (Invitrogen, Karlsruhe, Germany) under standard conditions at 37 °C in a humidified atmosphere containing 5 % $CO_2$ and 95 % air. Twenty-four hours before treatment, the cells were transferred to RPMI 1640 medium (Invitrogen, Karlsruhe, Germany) supplemented with 2.5 % charcoal-stripped FCS (PAN Biotech, Aldenbach, Germany) and 1 % PS. Heteronemin was dissolved in DMSO and diluted with medium (final DMSO concentration <0.1 %) to 1 and 5 µM. Experiments under each set of condition were carried out in triplicate. Blanks contained DMSO in the medium of the test compounds. After 18 h of incubation, ethoxyresorufin (final concentration 5.0 µM, Sigma-Aldrich, Munich, Germany) was added and 0.4 ml aliquots of the medium were sampled after 60 and 200 min. Subsequently, the formation of resorufin was analysed by spectrofluorometry (PerkinElmer LS50B, Waltham, MA, USA) with an excitation wavelength of 530 nm and an emission wavelength of 585 nm.

### Adhesion assay

MCF-7 cells ($1.5 \times 10^4$ cells/well) were seeded in serum-free medium (DMEM containing 0.5 % BSA, 2 mM $CaCl_2$, and 2 mM $MgCl_2$). Then, CytoTracker™ (500× CytoTracker™ Solution from CytoSelect™ tumour-endothelium adhesion assay from Cell Biolabs, Inc., San Diego, CA, USA, CBA-215) was added to the cell suspension, incubated for 1 h at 37 °C, and centrifuged at 1,000 rpm for 2 min. Then, the medium was aspirated, the cell pellet was washed 3× with serum-free medium (DMEM containing 0.5 % BSA, 2 mM $CaCl_2$, and 2 mM $MgCl_2$), and then the cell pellet was re-suspended in EGM2 MV medium. Meanwhile, the medium was aspirated from the endothelial cell culture (in wells of a 48-well plate), collected in Eppendorf tubes, and either heteronemin or DMSO (Sigma-Aldrich, Munich, Germany) was added. Then, the medium was re-distributed to LEC layers and incubated for 10 min. Also, the MCF-7 cell suspension, which was stained with CytoTracker™, was treated with heteronemin or DMSO and incubated for 10 min at room temperature. Furthermore, the medium was aspirated from the 48-well plate, and 200 µl of treated MCF-7 cell suspension was added to each well containing LECs grown in monolayers and incubated for 40 min at 37 °C. Then, the medium was aspirated from each well and washed 3× with 250 µl 1× Wash Buffer (10× Wash Buffer was from CytoSelect™ tumour-endothelium adhesion assay). Before the third wash, cells were inspected for morphological changes under the microscope. Then, the final wash was aspirated, and the plate was tapped on a flint-free paper towel; 150 µl of 1× Lysis Buffer (4× Lysis Buffer were from CytoSelect™ tumour-endothelium adhesion assay) was added to each well and lysed by the shearing forces through a pipette tip; 100 µl of the lysate was transferred to a 96-well clear bottom plate, and then, the fluorescence was read with a fluorescence plate reader at 485/530 nm.

### 12(S)-HETE assay

MCF-$7^{ALOX12}$ cells (MCF-$7^{VEGF\text{-}C/80/1/2ALOX15\text{-}}$pTAG-ALOX12-V5 cells; Kerjaschki et al. 2011), which were cultivated in MEM medium (Gibco # 10370-047) supplemented with 10 % FCS (foetal calf serum), 1 % GlutaMAX™-I (Gibco #35050-038), 1 % penicillin/streptomycin (Gibco #15140-148), 1 mg/ml G148-sulphate (PAA, #P25-011), 150 µg/ml hygromycin B (Sigma-Aldrich, #H3274), and 1 µg/ml puromycin, were seeded in 3.5-cm dishes and grown in 2.5 ml complete MEM medium without selection pressure. The next day, the medium was changed for serum-free medium and cells were kept at 37 °C for 24 h. Then, cells were treated with 10 µM arachidonic acid (#A3555, Sigma-Aldrich, St. Louis, MO 63103 USA) and simultaneously with different concentrations of the indicated compounds for 4 h when the supernatants were aspirated, centrifuged at 2000 rpm at 4 °C for 5 min. Then, 1.25 ml of medium samples were passed through extraction cartridges (Oasis™ HLB 1 cc, Waters, Milford, MA; equilibrated with 2 × 1 ml methanol, 2 × 1 ml distilled $H_2O$ immediately before use) followed by washing of cartridges with 3 × 1 ml distilled $H_2O$. Bound 12(S)-HETE was eluted with 500 µl methanol.

After the evaporation of methanol with a Speedvac concentrator, the samples were reconstituted with 250 µl assay buffer of the 12(S)-HETE enzyme immunoassay kit (EIA, # ADI-900-050; Enzo Life Sciences, Lausen, Switzerland), and sample volumes of 100 µl each (diluted 1:54) were subjected to 12(S)-HETE analysis according to the manufacturers' instructions (Kretschy et al. 2013; Viola et al. 2013b). Absorbance was measured with a Wallac 1420 Victor2 multilabel plate reader (Perkin Elmer Life and Analytical Sciences).

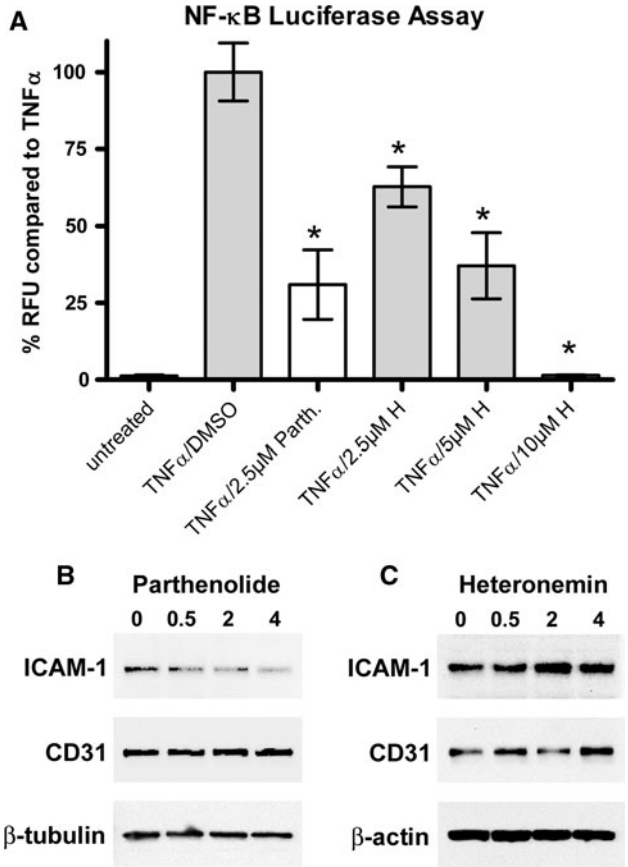


**Fig. 2** **a** Effect of heteronemin on NF-κB activation. $10 \times 10^6$ HEK293-NFκB-Luc cells were transfected with an expression plasmid for green fluorescence protein. After incubation for 6 h, $4 \times 10^4$ cells per well were seeded in serum- and phenol red-free DMEM in a 96-transparent-well plate. On the next day, cells were treated with indicated drug concentrations, 2.5 µM parthenolide (Parth.) as a specific inhibitor of NF-κB, heteronemin (H), or solvent vehicle (DMSO; untreated). One hour after treatment, cells were stimulated with 2 ng/ml human recombinant TNFα for additional 4 h. Luminescence of the firefly luciferase and fluorescence of the GFP were quantified on a GeniusPro plate reader. The luciferase signal derived from the NF-κB reporter was normalised by the GFP-derived fluorescence to account for differences in cell number or transfection efficiency. Experiments were performed in triplicate. *Asterisks* indicate significance compared to untreated control ($p < 0.05$), and *error bars* indicate mean ± SEM. Analysis of adherence protein expression. LECs were treated with **b** 5 µM parthenolide **c** 5 µM heteronemin for the indicated times. After cells were harvested, the protein lysates were analysed by Western blotting using the indicated antibodies. Solvent-treated LECs were used as negative control and β-actin and β-tubulin analyses served as loading control

## Statistical analysis

For statistical analyses, Excel 2003 software and Prism 5 software package (GraphPad, San Diego, CA, USA) were used. The values were expressed as mean ± SEM, and the Student's *t* test was applied to compare differences between control samples and treatment groups. Statistical significance level was set to $p < 0.05$.

# Results

## Heteronemin inhibits CCID formation

The pro-apoptotic and anti-inflammatory sesterterpene heteronemin was tested regarding anti-metastatic properties. A reductionistic co-culture model resembles the intravasation of tumour emboli (represented by MCF-7 breast cancer cell spheroids) into the lymphatic vasculature (mimicked by LEC monolayers) (Madlener et al. 2010; Kerjaschki et al. 2011; Vonach et al. 2011; Viola et al. 2013a). MCF-7 cells secrete 12(S)-HETE, which induces rapid and directional LEC migration, resulting in a radial cell-free radial zone in the lymph-endothelial cell monolayer directly underneath the MCF-7 spheroid, so-called

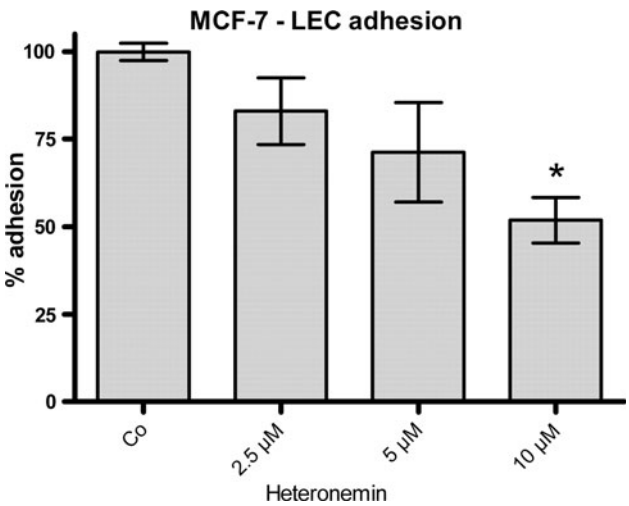


**Fig. 3** Cell adhesion assay. Trypsinised and cytotracker-stained MCF-7 cells were placed on LEC monolayers that were pre-treated with increasing concentrations of heteronemin. After 40 min, cells were washed and the percentages of MCF-7 cells that adhered to LECs were determined by measuring the fluorescence at 485/530 nm in the mixed cell lysate. Experiments were performed in triplicate. *Asterisks* indicate significance compared to untreated control ($p < 0.05$), and *error bars* indicate mean ± SEM

CCID. CCIDs can be considered as entry gates for tumour emboli on their way colonising lymph node after lymph node, which is a critical and probably rate limiting step for distant organ metastasis of ductal breast cancer (Kerjaschki et al. 2011). CCIDs can be attenuated by baicalein, a specific inhibitor of ALOX12/15, which causes the subsequent decrease in the 12(S)-HETE level. Hence, to control the contribution of this mechanism on CCID formation, the inhibitory effect of baicalein is shown in Fig. 1. Also, increasing concentrations of heteronemin inhibited CCID formation dose dependently (Fig. 1). Notably, the treatment of cells with heteronemin was not toxic at the used concentrations and for the indicated times (data not shown). CCID formation was recently shown to depend also on NF-κB activity, which can be inhibited by the *bona fide* NF-κB inhibitors Bay11-7082 and parthenolide. Figure 1 demonstrates the attenuation of CCID formation by Bay11-7082 and parthenolide, which were used as additional positive controls. For this reason, cells were also subjected to treatment with proadifen, which is a known inhibitor of CYPs and shown to inhibit CCID formation (Kretschy et al. 2013; p. 14). Such as pathernolide also heteronemin strongly repressed TNFα-induced activation of a NF-κB-driven luciferase reporter in HEK293 cells (Fig. 2a), which was consistent with recently published data (Schumacher et al. 2010). This suggested that NF-κB inhibition might be the mechanism responsible for the inhibition of CCID formation by heteronemin. However, in HUVECs, TNFα-induced selectin-E (SELE) expression, which is specific for NF-κB activation in endothelial cells, was not inhibited by heteronemin (Table 1). In LECs, ICAM-1 expression depends on NF-κB activity (Viola et al. 2013a), and thus, inhibition of NF-κB by parthenolide inhibits ICAM-1 (Fig. 2b) and CCIDs (Fig. 1). Interestingly, heteronemin slightly induced ICAM-1 expression in LECs (Fig. 2c), and hence, this finding did not support the hypothesis that heteronemin inhibited NF-κB in LECs. In contrast, the presented data rather suggest that the inhibition of NF-κB activation by heteronemin, which was evident in HEK293 cells, was hampered in LECs (Fig. 2c) and HUVECs (Table 1).

## Heteronemin reduces the adhesion of LECs to MCF-7 cells

Adhesion of MCF-7 spheroids to LECs is necessary to induce their retraction, and this movement is a prerequisite for CCID formation. Furthermore, ICAM-1 was shown to contribute to both adhesion and CCIDs (Viola et al. 2013a). Although heteronemin even induced ICAM-1 expression in LECs, the adhesion of MCF-7 cells to LECs was inhibited (Fig. 3), and the dose–response roughly correlated with the inhibition of CCID formation. CD31 is another prominent mediator of cell adhesion. However, also the expression of CD31 in LECs was not inhibited by heteronemin (Fig. 2c).

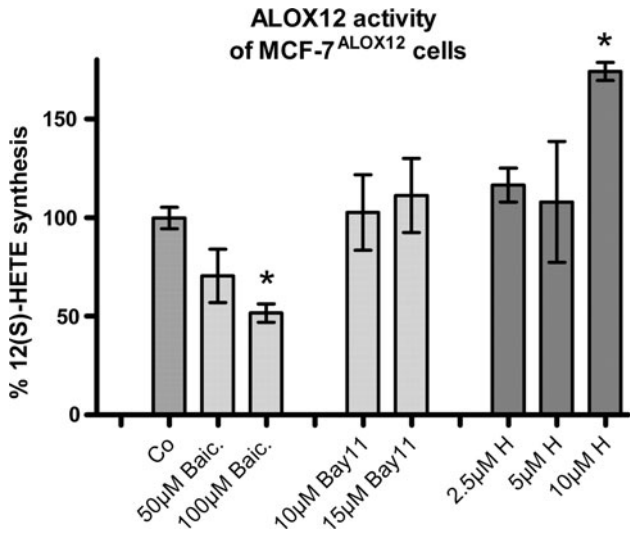


**Fig. 4** Effect of heteronemin on 12(S)-HETE synthesis. MCF-7$^{ALOX12}$ cells were seeded in 3.5-cm dishes and grown to 70 % confluence and treated with 10 μM arachidonic acid together with baicalein (Baic.), Bay11-7082 (Bay11) or heteronemin (H) for 4 h. DMSO was used as control (Co). The 12(S)-HETE concentration in the cell culture supernatant was determined by EIA. Experiments were performed in triplicate, and *error bars* indicate mean ± SEM and asterisks significance ($p < 0.05$)

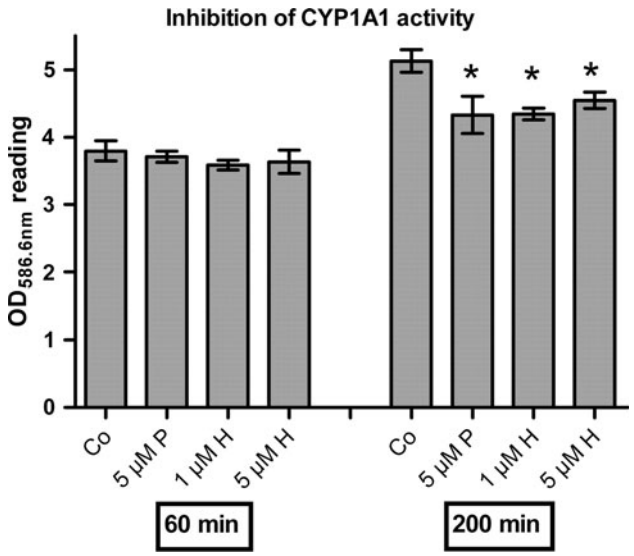


**Fig. 5** Inhibition of CYP1A1 activity in MCF-7 cells. MCF-7 cells were kept under steroid-free conditions and treated with 5 μM proadifen (P), 1 μM and 5 μM heteronemin (H), or solvent (DMSO; Co) for 18 h. Then, 5 μM ethoxyresorufin was added, and after 60 and 200 min, the formation of resorufin was analysed, which is specific for CYP1A1 activity. Experiments were done in triplicate, and *error bars* indicate mean ± SEM and *asterisks* significance ($p < 0.05$). No toxic effects were observed within the experimental setting

Therefore, the loss of adhesion induced by heteronemin was independent of ICAM-1 and CD31.

### Heteronemin does not inhibit 12(S)-HETE synthesis

Since 12(S)-HETE, which is produced by MCF-7 spheroids, is a trigger of CCIDs, the *bona fide* ALOX12/15 inhibitor baicalein inhibited CCID formation (Fig. 1). Hence, it was tested whether heteronemin also inhibits 12(S)-HETE synthesis in MCF-7 cells. For this, MCF-$7^{ALOX12}$ cells were treated with 10 μM arachidonic acid to provide ALOX12 with sufficient substrate and to drive the synthesis of 12(S)-HETE, which was measured by 12(S)-HETE EIA in presence and absence of inhibitors. Whereas baicalein dose dependently inhibited 12(S)-HETE synthesis heteronemin even induced the synthesis of 12(S)-HETE in MCF-$7^{ALOX12}$ cells (Fig. 4) despite inhibition of CCID formation. Hence, heteronemin did not attenuate CCIDs as a consequence of ALOX12 inhibition.

### Heteronemin inhibits CYP1A1 activity

Another mechanism playing a role in CCID formation involves cytochrome P450 enzymes (CYPs), because the CYP inhibitor proadifen (SKF525A) down-regulates paxillin (Kretschy et al. 2013), thereby inhibiting LEC plasticity and CCID formation (Fig. 1). Hence, heteronemin was tested regarding anti-CYP1A1 activity, because this cytochrome P450 family member was reported to contribute to breast cancer metastasis (Jiang et al. 2007); 1–5 μM heteronemin, as well as proadifen, significantly inhibited CYP1A1 activity as determined by EROD assay (Fig. 5), and therefore, the inhibition of CYP1A1 most likely contributed to heteronemin-mediated size reduction in CCIDs.

### Heteronemin suppresses paxillin levels

Next, markers indicating EMT and motility were analysed because it was shown that 12(S)-HETE induces this process in LECs (Vonach et al. 2011). For this, the pro-migratory stimulus produced by MCF-7 spheroids was replaced by synthetic 12(S)-HETE facilitating the analysis of protein expression/activation by Western blotting. The increased phosphorylation of MYPT (myosin-binding subunit of myosin phosphatase) and the expression of S100A4 by 1 μM 12(S)-HETE were not inhibited by 5 μM heteronemin (Fig. 6), implicating that the increased plasticity of LECs remained unchanged despite heteronemin treatment. Notably, however, heteronemin suppressed paxillin levels to below the level of detection. Paxillin was reported to be essential for the maintenance of labile adhesions and for the turnover of focal adhesion plaques, thereby facilitating rapid cell migration (Huang et al. 2003). Interestingly, the CYP inhibitor proadifen was also shown to inhibit paxillin expression (Kretschy et al. 2013). The transient de-phosphorylation of Erk1/2 upon 12(S)-HETE treatment was augmented by heteronemin and could be a consequence of repressed paxillin levels, because paxillin signals through the MAP kinase pathway (Deakin and Turner 2008).

## Discussion

Heteronemin, a natural compound derived from a marine sponge, was investigated regarding its activity interfering with the disintegration of the lymph-endothelial barrier triggered by 12(S)-HETE secreted by breast cancer emboli. At low micromolar concentrations, heteronemin attenuated CCID formation, which resembles a crucial step in cancer cell transmigration in and out of the lymphatic vasculature. Apart from the expression of ALOX12/15 and its product 12(S)-HETE, additional mechanisms are required to generate CCIDs, such as intercellular adhesion between tumour cells and lymph endothelium. Furthermore, the inhibition of cytochrome P450 (Kretschy et al. 2013), GTPases (Madlener et al. 2010), or NF-κB (Vonach et al. 2011; Viola et al. 2013a) attenuates the retraction of LECs and, therefore, the formation of CCIDs. Some of the mechanisms are independent of each other, or cross-talking, or upstream/downstream of the same signalling pathway.

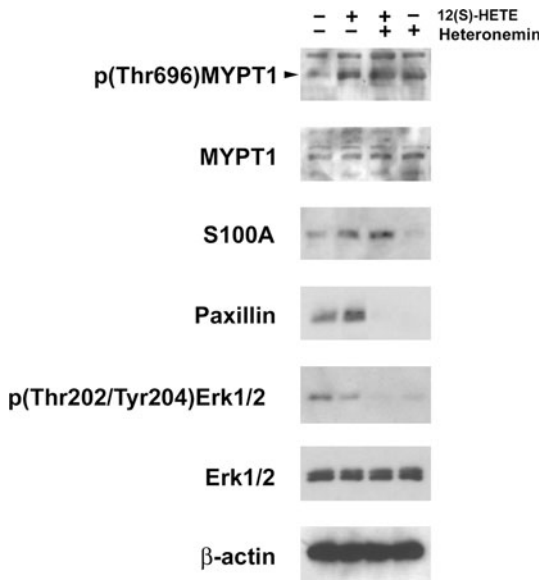


**Fig. 6** Analysis of protein expression. LECs were pre-treated with 5 μM heteronemin for 20 min and stimulated afterwards with 1 μM 12(S)-HETE for 60 min. Then, cells were harvested and the protein lysates analysed by Western blotting. Solvent-treated LECs were used as negative control, β-actin analysis served as loading control

Heteronemin strongly inhibited NF-κB activation in HEK293 cells. This effect of heteronemin was first shown in Jurkat and K562 cells (Schumacher et al. 2010), but could not be observed in HUVECs. Also, the expression of ICAM-1 in LECs, which depends on NF-κB, was not inhibited by heteronemin. In contrast, the specific NF-κB inhibitors parthenolide and Bay11-7082 caused the down-regulation of ICAM-1, which correlated with the adhesion of MCF-7 cells to LECs (Viola et al. 2013a). Interestingly, heteronemin even induced the expression of ICAM-1 and CD31 in LECs, although the adhesion between MCF-7 cells and LECs was significantly reduced. This indicated that attenuation of CCID formation by heteronemin was independent of ICAM-1, CD31, and NF-κB.

The formation of CCIDs depends on the mobility and directional migration of LECs in the opposite direction of the 12(S)-HETE gradient ("retraction factor", Honn et al. 1994) secreted by MCF-7 cells. Hence, the expression of mobility proteins was investigated in LECs. Previous experiments could associate the phosphorylated state of MYPT with the mobile phenotype in LECs (Kerjaschki et al. 2011). MYPT1, the regulatory/targeting subunit of the myosin phosphatase, is activated by 12(S)-HETE and regulates the interaction of actin and myosin in response to signalling through the GTPase Rho (Feng et al. 1999). Therefore, the process that is triggered by 12(S)-HETE seems to directly signal downstream to LECs inducing Rho, MYPT, and migration. However, heteronemin did not abrogate MYPT activation, and therefore, it was unlikely that heteronemin targeted the Rho-MYPT pathway. Heteronemin caused even an increase in MYPT phosphorylation, which was probably due to the increase in the 12(S)-HETE level in MCF-7 cells. Also, the CYP inhibitor proadifen, which inhibits CCID formation, induces the level of 12(S)-HETE in MCF-7 cells (Kretschy et al. 2013), because both, CYP and ALOX12, utilise and compete for arachidonic acid as their major substrate and are therefore cross-talking. Hence, the inhibition of one enzyme (i.e. CYP) by heteronemin or proadifen provides more substrate for the respective other enzyme (ALOX12) resulting in increased levels of its metabolite 12(S)-HETE. This implicates that the CCID-inhibitory mechanism(s) of heteronemin and proadifen (through the inhibition of CYP) prevail over the counteracting induction of 12(S)-HETE. CYP1A1, a member of the cytochrome P450 family, was shown to play a role in breast cancer metastasis (Jiang et al. 2007), and therefore, this very property of heteronemin needs to be addressed in more detailed studies.

Five micromolar heteronemin completely blocked paxillin expression in LECs, and it is of note that, besides proadifen, also xanthohumol inhibited paxillin expression and CYP activity (Viola et al. 2013b). Paxillin is a prominent molecule regulating cell polarity (Digman et al. 2008), controls adhesion plaque function, and labile adhesions facilitating rapid endothelial cell migration across the substratum (Huang et al. 2003; Deakin and Turner 2008). These properties are essential for directed cell movement (West et al. 2001; Jianxin et al. 2009) and hence CCID formation.

Interestingly, the expression of paxillin in endothelial cells is also required for the transmigration of neutrophils through the endothelial barrier, and thus, endothelial paxillin influences the behaviour of other cell types that are in direct contact with endothelial cells (Parson et al. 2012). Suppression of paxillin is indicative for the acquisition of an epithelial, more differentiated phenotype (Paulitschke et al. 2010; Lu et al. 2006; van Zijl et al. 2011).

In conclusion, we describe three distinct properties of heteronemin affecting CCID formation:

1. The inhibition of CYP1A1 in MCF-7 cells.
2. The reduction in cell–cell adhesion, which was possibly due to the inhibition of NF-κB in MCF-7 cells (Vonach et al. 2011) but not in LECs and HUVECs, because SELE, CD31, and ICAM-1 remained expressed (Viola et al. 2013a).
3. The repression of paxillin in LECs, which is a major regulator of focal adhesions and directional cell migration (Paulitschke et al. 2010, Deakin and Turner 2008).

Hence, heteronemin, which effectively reduced the lymph-intravasating properties of MCF-7 spheroids, should undergo in vivo scrutiny.

**Acknowledgments** We wish to thank Toni Jäger for preparing the figures and to Prof Ulrichova for kindly providing HUVEC cells. Heteronemin was a kind gift of Professor Marcel Jaspars (University of Aberdeen) and was originally obtained from the NCI open repository. This work was supported by the Austrian Science Fund, FWF, grant number P20905-B13 (to W.M.), and grant numbers S10704-B03 and S10704-B13 (to V.M.D.), by the European Union, FP7 Health Research, project number HEALTH-F4-2008-202047 (to W.M.), further by a grant of the Fellinger foundation (to G.K.), grants of the Herzfelder family foundation (to T.S., H.D., P.S. and M.G.), a grant of the "Hochschuljubilaeumsstiftung der Stadt Wien" grant number H-2498/2011 (to P.S.), a scholarship from the Austrian exchange service OeAD (to K.J.). Grant Agency of the Czech Republic GACR (P505/11/1163) and ED0007/01/01 (to L.R. and M.S) from the Centre of the Region Haná for Biotechnological and Agricultural Research is also gratefully acknowledged.

**Conflict of interests** None.

## References

Carlson RW, Allred DC, Anderson BO, Burstein HJ, Carter WB, Edge SB, Erban JK, Farrar WB, Goldstein LJ, Gradishar WJ, Hayes DF, Hudis CA, Jahanzeb M, Kiel K, Ljung BM, Marcom PK, Mayer IA, McCormick B, Nabell LM, Pierce LJ, Reed EC, Smith ML, Somlo G, Theriault RL, Topham NS, Ward JH,

Winer EP, Wolff AC (2009) Breast cancer. Clinical practice guidelines in oncology. NCCN Breast cancer clinical practice guidelines panel. J Natl Compr Canc Netw 7(2):122–192

Cragg GM, Newman DJ, Yang SS (2006) Natural product extracts of plant and marine origin having antileukemia potential. The NCI experience. J Nat Prod 69(3):488–498

Deakin NO, Turner CE (2008) Paxillin comes of age. J Cell Sci 121(15):2435–2444

Digman MA, Brown CM, Horwitz AM, Mantulin WW, Gratton E (2008) Paxillin dynamics measured during adhesion assembly and disassembly by correlation spectroscopy. Biophys J 94(7):2819–2831

Feng J, Masaaki I, Ichikawa K, Isaka N, Nishikawa M, Hartshorne DJ, Nakano T (1999) Inhibitory phosphorylation site for rho-associated kinase on smooth muscle myosin phosphatase. J Cell Biol 274:37385–37390

Folmer F, Jaspars M, Solano G, Cristofanon S, Henry E, Tabudravu J, Black K, Green DH, Küpper FC, Aalbersberg W, Feussner K, Dicato M, Diederich M (2009) The inhibition of TNF-α induced NF-κB activation by marine natural products. Biochem Pharmacol 78:592–606

Giessrigl B, Yazici G, Teichmann M, Kopf S, Ghassemi S, Atanasov AG, Dirsch VM, Grusch M, Jäger W, Özmen A, Krupitza G (2012) Effects of scrophularia extracts on tumor cell proliferation, death and intravasation through lymphendothelial cell barriers. Int J Oncol 40(6):2063–2074

Gridling M, Stark N, Madlener S, Lackner A, Popescu R, Benedek B, Diaz R, Tut FM, Vo NTP, Huber D, Gollinger M, Saiko P, Özmen A, Mosgoeller W, de Martin R, Eytner R, Wagner KH, Grusch M, Fritzer-Szekeres M, Szekeres T, Kopp B, Frisch R, Krupitza G (2009) In vitro anti-cancer activity of two ethnopharmacological healing plants from Guatemala *Pluchea odorata* and *Phlebodium decumanum*. Int J Oncol 34(4):1117–1128

Grusch M, Polgar D, Gfatter S, Leuhuber K, Huettenbrenner S, Leisser C, Fuhrmann G, Kassie F, Steinkellner H, Smid K, Peters GJ, Jayaram H, Klepal T, Szekeres T, Knasmüller S, Krupitza G (2002) Maintenance of ATP favours apoptosis over necrosis triggered by benzamide riboside. Cell Death Differ 9:169–178

Honn KV, Tang DG, Grossi I, Duniec ZM, Timar J, Renaud C, Leithauser M, Blair I, Johnson CR, Diglio CA et al (1994) Tumour cell-derived 12(S)-hydroxyeicosatetraenoic acid induces microvascular endothelial cell retraction. Cancer Res 54:565–574

Huang C, Rajfur Z, Borchers C, Schaller MD, Jacobson K (2003) JNK phosphorylates paxillin and regulates cell migration. Nature 424:219–223

Jiang JG, Ning YG, Chen C, Ma D, Liu ZJ, Yang S, Zhou J, Xiao X, Zhang XA, Edin ML, Card JW, Wang J, Zeldin DC, Wang DW (2007) Cytochrome p450 epoxygenase promotes human cancer metastasis. Cancer Res 67(14):6665–6674

Jianxin AY, Deakin NO, Turner CE (2009) Paxillin-kinase-linker tyrosine phosphorylation regulates directional cell migration. Mol Biol Cell 20(22):4706–4719

Kerjaschki D, Bago-Horvath Z, Rudas M, Sexl V, Schneckenleithner C, Wolbank S, Bartel G, Krieger S, Kalt R, Hantusch B, Keller T, Nagy-Bojarszky K, Huttary N, Raab I, Lackner K, Krautgasser K, Schachner H, Kaserer K, Rezar S, Madlener S, Vonach C, Davidovits A, Nosaka H, Hämmerle M, Viola K, Dolznig H, Schreiber M, Nader A, Mikulits W, Gnant M, Hirakawa S, Detmar M, Alitalo K, Nijman S, Offner F, Maier TJ, Steinhilber D, Krupitza G (2011) Lipoxygenase mediates invasion of intrametastatic lymphatic vessels and propagates lymph node metastasis of human mammary carcinoma xenografts in mouse. J Clin Invest 121(5):2000–2012

Kobayashi M, Okamoto T, Hayashi K, Yokoyama N, Sasaki T, Kitagawa I (1994) Marine natural products. XXXII. Absolute configurations of C-4 of the manoalide family, biologically active sesterterpenes from the marine sponge *Hyrtios erecta*. Chem Pharm Bull (Tokyo) 42(2):265–270

Kretschy N, Teichmann M, Kopf S, Atanasov AG, Saiko P, Vonach C, Viola K, Giessrig B, Huttary N, Raab I, Krieger S, Jäger W, Szekeres T, Nijman SM, Mikulits W, Dirsch VM, Dolznig H, Grusch M, Krupitza G (2013) In vitro inhibition of breast cancer spheroid-induced lymphendothelial defects resembling intravasation into the lymphatic vasculature by acetohexamide, isoxsuprine, nifedipine and proadifen. Br J Cancer 108(3):570–578

Leung HWC, Yang WH, Lai MY, Lin CJ, Lee HZ (2007) Inhibition of 12-lipoxygenase during baicalein-induced human lung non-small carcinoma H460 cell apoptosis. Food Chem Toxicol 45:403–411

Lu H, Murtagh J, Schwartz EL (2006) The microtubule binding drug laulimalide inhibits vascular endothelial growth factor-induced human endothelial cell migration and is synergistic when combined with docetaxel (taxotere). Mol Pharmacol 69(4):1207–1215

Madlener S, Svacinová J, Kitner M, Kopecky J, Eytner R, Lackner A, Vo NTP, Frisch R, Grusch M, de Martin R, Dolezal K, Strnad M, Krupitza G (2009) In vitro anti-inflammatory and anticancer activities of extracts of *Acalypha alopecuroidea* (Euphorbiaceae). Int J Oncol 35(4):881–891

Madlener S, Saiko P, Vonach C, Viola K, Huttary N, Stark N, Popescu R, Gridling M, Vo NT, Herbacek I, Davidovits A, Giessrigl B, Venkateswarlu S, Geleff S, Jäger W, Grusch M, Kerjaschki D, Mikulits W, Golakoti T, Fritzer-Szekeres M, Szekeres T, Krupitza G (2010) Multifactorial anticancer effects of digalloyl-resveratrol encompass apoptosis, cell-cycle arrest, and inhibition of lymphendothelial gap formation in vitro. Br J Cancer 102(9):1361–1370

Nie D, Honn KV (2004) Eicosanoid regulation of angiogenesis in tumors. Semin Thromb Hemost 30:119–125

Nie D, Nemeth J, Qiao Y, Zacharek A, Li L, Hanna K, Tang K, Hillman GG, Cher ML, Grignon DJ, Honn KV (2003) Increased metastatic potential in human prostate carcinoma cells by overexpression of arachidonate 12-lipoxygenase. Clin Exp Metast 20:657–663

Orlowski RZ, Baldwin AS Jr (2002) NF-κB as a therapeutic target in cancer. Trends Mol Med 8(8):385–389

Paulitschke V, Schicher N, Szekeres T, Jäger W, Elbling L, Riemer AB, Scheiner O, Trimurtulu G, Venkateswarlu S, Mikula M, Swoboda A, Fiebiger E, Gerner C, Pehamberger H, Kunstfeld R (2010) 3,3′,4,4′,5,5′-Hexahydroxystilbene impairs melanoma progression in a metastatic mouse model. J Invest Derm 130(6):1668–1679

Rice RL, Tang DG, Hddadi M, Honn KV, Taylor JD (1998) 12(S)-Hydroxyeicosatetraenoic acid increases microfilament content in B16a melanoma cells: a protein kinase-dependent process. Int J Cancer 77:271–278

Schoppmann SF, Soleiman A, Kalt R, Okubo Y, Benisch C, Nagavarapu U, Herron GS, Geleff S (2004) Telomerase-immortalized lymphatic and blood endothelial cells are functionally stable and retain their lineage specificity. Microcirculation 11:261–269

Schumacher M, Cerella C, Eifes S, Chateauvieux S, Morceau F, Jaspars M, Dicato M, and Diederich M (2010) Heteronemin, a spongean sesterterpene, inhibits TNF alpha-induced NF-kappa B activation through proteasome inhibition and induces apoptotic cell death. Biochem Pharmacol 79(4):610–622 Epub. Erratum in: Biochem Pharmacol 2010 79(12):1837

Sobin LH, Gospodarowicz MK, Wittekind C (eds) (2009) TNM classification of malignant tumours (Uicc International Union Against Cancer). Wiley-Blackwell, New York

Spector AA, Gordon JA, Moore SA (1988) Hydroxyeicosatetraenoic acids (HETEs). Prog Lipid Res 27:271–323

Tang DG, Timar J, Grossi IM, Renaud C, Kimler VA, Diglio CA, Taylor JD, Honn KV (1993) The lipoxygenase metabolite, 12(S)-HETE, induces a protein kinase C-dependent cytoskeletal rearrangement and retraction of microvascular endothelial cells. Exp Cell Res 207:361–375

Uchide K, Sakon M, Ariyoshi H, Nakamori S, Tokunaga M, Monden M (2007) Cancer cells cause vascular endothelial cell retraction via 12(S)-HETE secretion; the possible role of cancer cell derived microparticle. Ann Surg Oncol 14:862–868

van Zijl F, Krupitza G, Mikulits W (2011) Initial steps of metastasis: cell invasion and endothelial transmigration. Rev Mutat Res 728(1–2):23–34

Viola K, Kopf S, Huttary N, Vonach C, Kretschy N, Teichmann M, Giessrigl B, Raab I, Stary S, Krieger S, Keller T, Bauer S, Hantusch B, Szekeres T, de Martin R, Jäger W, Mikulits W, Dolznig H, Krupitza G, Grusch M (2013a) Bay11-7082 inhibits the disintegration of the lymphendothelial barrier triggered by MCF-7 breast cancer spheroids; the role of ICAM-1 and adhesion. Br J Cancer 108(3):564–569

Viola K, Kopf S, Rarova L, Jarukamjorn K, Kretschy N, Teichmann M, Vonach C, Atanasov AG, Giessrigl B, Huttary N, Raab I, Krieger S, Strnad M, de Martin R, Saiko P, Szekeres T, Knasmüller S, Dirsch VM, Jäger W, Grusch M, Dolznig H, Mikulits W, Krupitza G (2013b) Xanthohumol attenuates tumor cell-mediated breaching of the lymphoendothelial barrier and prevents intravasation and metastasis. Arch Toxicol [Epub ahead of print]

Vonach C, Viola K, Giessrigl B, Huttary N, Raab I, Kalt R, Krieger S, Vo NTP, Madlener S, Bauer S, Marian B, Hämmerle M, Kretschy N, Teichmann M, Hantusch B, Stary S, Unger C, Seelinger M, Eger A, Mader R, Jäger W, Schmidt W, Grusch M, Dolznig H, Mikulits W, Krupitza G (2011) NF-κB mediates the12(S)-HETE-induced endothelial to mesenchymal transition of lymphendothelial cells during the intravasation of breast carcinoma cells. Br J Cancer 105(2):263–271

West KA, Zhang H, Brown MC, Nikolopoulos SN, Riedy MC, Horwitz AF, Turner CE (2001) The LD4 motif of paxillin regulates cell spreading and motility through an interaction with paxillin kinase linker (PKL). J Cell Biol 154(1):161–176

Wonganuchitmeta SN, Yuenyongsawad S, Keawpradub N, Plubrukarn A (2004) Antitubercular sesterterpenes from the Thai sponge *Brachiaster* sp. J Nat Prod 7(10):1767–1770

Yoshimura R, Matsuyama M, Mitsuhashi M, Takemoto Y, Tsuchida K, Kawahito Y, Sano H, Nakatani T (2004) Relationship between lipoxygenase and human testicular cancer. Int J Mol Med 13:389–393

Zhang JS, Nelson M, Wang L, Liu W, Qian CP, Shridhar V, Urrutia R, Smith DI (1998) Identification and chromosomal localization of CTNNAL1, a novel protein homologous to alpha-catenin. Genomics 54:149–154